JOURNAL OF SOLID STATE CHEMISTRY 35, 128–132 (1980)

Preparation and Photoelectronic Properties of $FeNbO_4$

JOHN KOENITZER, BIJAN KHAZAI, JACOB HORMADALY,
ROBERT KERSHAW, KIRBY DWIGHT, AND AARON WOLD*

Department of Chemistry, Brown University, Providence,
Rhode Island 02912

Received January 30, 1980; in final form April 18, 1980

The orthorhombic α-PbO_2 phase of $FeNbO_4$ was prepared and its photoelectronic properties measured: Sintered disks were shown to be *n* type and gave a resistivity of 40 Ω-cm. Measurements of the photoresponse gave a flat-band potential between 0.1 and 0.4 V vs SCE at a pH of 8.5 and an optical band gap of 2.08(2) eV. Several higher-energy band gaps at 2.68(2), 2.94(2), 3.24(2), and 4.38(2) eV were also determined. There appears to be an enhancement of the quantum efficiency due to the presence of $[FeO_6]$ active centers while retaining the fundamental characteristics of the $[NbO_6]$ octahedra.

Introduction

The photoelectronic properties of $Ba_{0.5}Sr_{0.5}Nb_2O_6$ and $Sr_2Nb_2O_7$ have recently been investigated (*1*). Despite their different structures, both compounds contain a single photoactive $[NbO_6]$ center. It was shown that whereas the band gap and, probably, the quantum efficiency of ternary transition metal oxides containing similar $[MO_6]$ octahedra are structure dependent, the flat-band potential is influenced by the nature of the *A*-site ions. Another potentially interesting niobate would be the compound $FeNbO_4$ which crystallizes below 1085°C with the monoclinic wolframite structure. Between 1085 and 1380°C there is an order–disorder transition in which the separate chains of NbO_6 and FeO_6 octahedra in the wolframite structure become identical, and an orthorhombic α-PbO_2 phase is formed between 1380 and 1410°C. A further transition to the tetragonal rutile structure occurs in which the $(FeNb)O_6$ octahedra change from a zig-zag configuration in the (α-PbO_2) structure to straight chains in the rutile structure. It is well known (*2*) that if the sites occupied by M and M' in $MM'X_4$ ($FeNbO_4$) or MM'_2X_6 ($FeNb_2O_6$) are those occupied by M in MX_2, the more complex structures may be described as superstructures of the simpler MX_2 structures. Hence, in $FeNbO_4$ the octahedral sites between alternate pairs of close-packed layers in the α-PbO_2 structure are occupied by Fe and Nb atoms, and in the columbite structure there is a more complex type of replacement. However, in all of the structures, one-half of the octahedral sites are occupied in a hexagonal close-packed array of anions.

It has also been indicated by Turnock (*3*) that $FeNb_2O_6$ may be incorporated in solid solution with $FeNbO_4$. By this mechanism, one might expect that the resistivity of $FeNbO_4$ can be adjusted by the presence of

---

* To whom all correspondence should be addressed.

0022-4596/80/130128-05$02.00/0

controlled small concentrations of Fe^{2+}. The photoelectronic properties of "conducting" $FeNbO_4$ could then be measured and its suitability as an n-type photoanode determined. In addition, a comparison can be made with the properties of $Ba_{0.5}Sr_{0.5}Nb_2O_6$ and $Sr_2Nb_2O_7$ in order to ascertain the effect of adding a second photoactive center, namely, $[FeO_6]$ octahedra, to the $[NbO_6]$ center found in the two alkaline earth niobates.

Experimental Procedure

Synthesis

$FeNbO_4$ was prepared from the solid-state reaction between Fe_2O_3 (Johnson–Matthey, specpure) and Nb_2O_5 (Kawecki Berylco Industries, spectroscopic grade). A finely ground mixture of appropriate amounts of the starting materials was placed in a platinum crucible and heated at 1150°C for 48 hr. The sample was cooled, reground, and reheated for an additional 48 hr. The sample was X-rayed and then reheated; after a third heating, the product was cooled to room temperature in the furnace and reexamined by X-ray analysis. This was done in order to confirm the formation of a single phase. A Phillips Norelco diffractometer, with Cu$K\alpha$ radiation (1.5405 Å) at a scan rate of 0.25° 2θ min^{-1}, was used.

Disks were formed by pressing aliquots of approximately 150 mg at 90,000 psi; 5 drops of Carbowax was added to the powder before pressing in order to facilitate the formation of a well-sintered disk. The pressed disks were placed on platinum supports in a cold furnace. The disks were heated in a hollow globar furnace at a rate of 85°C per hour to 1330°C, and maintained at that temperature for 24 hr. At the end of the sintering process, the disks were cooled at the same rate. X-Ray diffraction patterns of the sintered disks showed, at the limit of detection, the presence of the strongest line of α-Fe_2O_3. This is consistent with the reduction of a small amount of Fe^{3+} to Fe^{2+} under the conditions of sintering. The resulting formation of $FeNb_2O_6$ in solution with $FeNbO_4$ gives rise to conductivity. Essentially identical resistivities were measured before and after abrading these disks to one-half their original thickness, which established their homogeneity.

Electrode Preparation

Photoanodes were prepared by evaporating thin films of gold on the backs of the disks to provide good electrical contact. The gold face of the disk was attached to a platinum wire by means of indium solder. Miccrostop (Michigan Chrome Chemical Corp.) was applied to the gold face and the electrode wire. The photoelectrolysis measurements were carried out with a 150-W xenon lamp, a monochromator (Oriel Model 7240), a glass cell with a quartz window, and a current amplifier as described previously (*6*). The electrolyte, 0.2 *M* sodium acetate (pH = 8.5), was purged of dissolved oxygen and stirred by continuous bubbling of 85% argon–15% hydrogen gas. Any abrasion of the exposed face of the disk had an adverse effect on the performance of the photoanode.

Results

The monoclinic α-PbO_2 phase of $FeNbO_4$ was prepared and X-ray analysis gave the following cell constants: $a = 5.000(1)$, $b = 5.622(2)$, $c = 4.652(1)$, $\beta = 89.84°$. The resistivities of the samples were measured using the Van der Pauw technique (*4*). Contacts were made by the ultrasonic soldering of indium directly onto the samples, and their ohmic behavior was established by measuring their current–voltage characteristics. The room-temperature resistivities of the disks were all 40 ± 1 Ω-cm.

The disks were proven to be *n*-type by qualitative measurement of the Seebeck effect. However, routine measurements were unable to detect any Hall voltage in these compounds, which indicates that their mobilities are less than 0.1 cm^2/V-sec, as would be expected for a hopping conductor (*5*). Given the above resistivity, the minimum carrier concentration, of the order of 2×10^{18} cm^{-3}, can then be estimated for the $FeNbO_4$ disks prepared. It would be anticipated that the resistivity of intrinsic $FeNbO_4$ would be much higher than 40 Ω-cm. As discussed earlier, Turnock (*3*) indicated that $FeNb_2O_6$ may be incorporated in solid solution with $FeNbO_4$. The formation of such solid solution would be consistent with relatively high conductivity and the phase separation of a few percent of α-Fe_2O_3. Careful examination of X-ray patterns of the $FeNbO_4$ powder indicated the existence of a single phase; however, those obtained from sintered disks showed the presence of the strongest peak of α-Fe_2O_3.

The photoresponse observed for $FeNbO_4$ is presented in Fig. 1, where the photocurrents obtained in "white" light are plotted against the anode potential measured with respect to a saturated calomel electrode (SCE). The general shape of this curve is similar to those reported for other iron compounds (*7*); the current continues to rise without any indication of saturation (bending over). Although the onset of photocurrent with increasing anode potential is not sufficiently abrupt for a determination of the flat-band potential, it would appear to lie in the range of 0.1 to 0.43V vs SCE. The presence of iron is known to increase the flat-band potential from −0.73 V for TiO_2 to 0.43 V for $FeTiO_3$ (*8*), both corrected to pH 8.5. A quantitatively similar shift occurs in the niobates. Photoresponse curves for $Ba_{0.5}Sr_{0.5}Nb_2O_6$ and $Sr_2Nb_2O_7$ have been included in Fig. 1 to demonstrate the comparison between $FeNbO_4$ and these other two niobates (*1*).

The quantum efficiency η (in electrons/photon) of $FeNbO_4$ measured at an anode potential of 0.8 V vs SCE is plotted against wavelength in Fig. 2. Analogous results for $Ba_{0.5}Sr_{0.5}Nb_2O_6$ and $Sr_2Nb_2O_7$ are again included for the purpose of comparison. The photoresponse of $FeNbO_4$ extends to considerably longer wavelengths than either of the other two

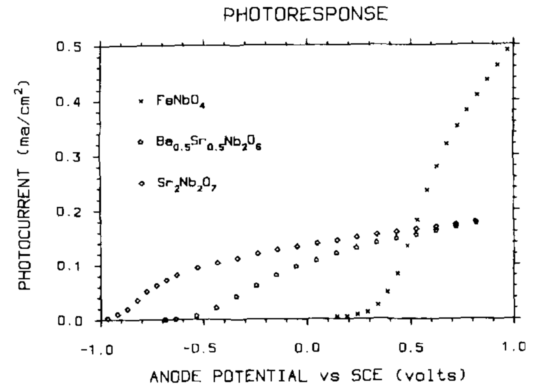

FIG. 1. Variation of photocurrent with anode potential for $FeNbO_4$ in 0.2 *M* sodium acetate (pH 8.5) under "white" xenon arc irradiation of 1.0 W/cm^2, as compared with analogous results for $Sr_2Nb_2O_7$ and $Ba_{0.5}Sr_{0.5}Nb_2O_6$.

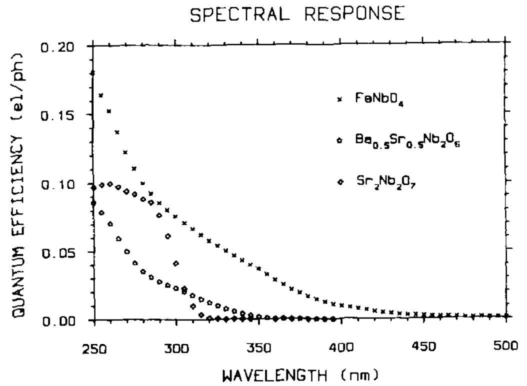

FIG. 2. Spectral variation of the quantum efficiency obtained for $FeNbO_4$ in 0.2 *M* sodium acetate at an anode potential of 0.8 V with respect to SCE, showing similarity to the analogous results for $Ba_{0.5}Sr_{0.5}Nb_2O_6$, but dissimilarity to those found for $Sr_2Nb_2O_7$.

niobates. Nevertheless, the shape of its spectral response curve bears striking resemblance to that obtained for $Ba_{0.5}Sr_{0.5}Nb_2O_6$.

It has been shown that such spectral response data can be analyzed so as to yield reliable values not only for the lowest optical band gap, but also for higher-energy transitions (*9*). Since these materials fulfill the required criteria (*9*), the observed quantum efficiency η was multiplied by the corresponding photon energy $h\nu$, and the square root of this quantity is shown as a function of photon energy in Fig. 3. These data yield a lowest-energy optical band gap of 2.08(2) eV, which is consistent with values between 2.1 and 2.2 eV reported for other iron compounds (*8*).

However, the data presented in Fig. 3 give evidence for the superposition of several additional band gaps at higher energies. These are indicated by the sudden increases in slope (*9*) which occur at 2.68(2), 2.94(5), 3.24(4), and 4.38(2) eV. Although the optical band gap at 2.08 eV is definitely indirect, these subsequent transitions are too closely spaced to permit reliable differentiation between direct and indirect character. Three of these values agree closely with the energy gaps of 2.6(1), 3.38(2), and 4.44(2) eV reported for $Ba_{0.5}Sr_{0.5}Nb_2O_6$. This agreement implies that the photoactive Fe^{3+} and Nb^{5+} centers retain at least some of their individuality; the overall band structure appears to approximate a sum rather than an average.

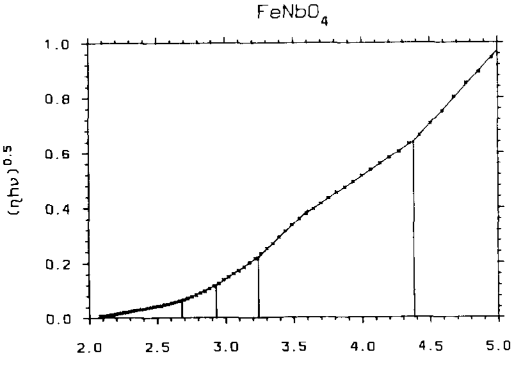

FIG. 3. Indirect band gap analysis for $FeNbO_4$, showing an optical band gap of 2.08 eV. The presence of additional band edges at 2.68, 2.93, 3.24, and 4.38 eV is indicated by sudden increases in the slope of the curve at these energies.

The differences between the energy gaps of 3.36 and 3.86 eV obtained for the pyrochlore $Sr_2Nb_2O_7$ and those of the perovskite $Ba_{0.5}Sr_{0.5}Nb_2O_6$ were attributed to structural effects. Our present findings suggest that it is the degree of occupancy of the *A* site which may be important. In $FeNbO_4$, the Fe^{3+} and Nb^{5+} ions occupy *B*-site octahedra; all the *A* sites are vacant. the resulting niobium-related energy gaps are similar to those of the $Ba_{0.5}Sr_{0.5}Nb_2O_6$ where half of the *A* sites remain vacant, but distinct from those of $Sr_2Nb_2O_7$ where all the *A* sites are filled.

Summary and Conclusions

The orthorhombic α-PbO_2 phase of $FeNbO_4$ was prepared. Disks, sintered in a hollow globar furnace, were shown to be *n* type and gave a resisitivity of 40 Ω-cm. This conductivity undoubtedly arises from the incorporation of a small amount of $FeNb_2O_6$ in solid solution with $FeNbO_4$ (*3*).

Measurement of the photoresponse of this material indicates a flat-band potential between 0.1 and 0.4 V vs SCE in a pH of 8.5, an optical band gap of 2.08(2) eV, and the superposition of several higher-energy band gaps at 2.68(2), 2.94(2), 3.24(2), and 4.38(2) eV. (The decrease in slope (Fig. 3) resembles that seen in $SrTiO_3$ at 3.5 eV and does not represent a higher-energy transition.)

These results were compared with the properties of reduced $Ba_{0.5}Sr_{0.5}Nb_2O_6$ and $Sr_2Nb_2O_7$. The observed shift in flat-band potential between these two niobates and $FeNbO_4$ agrees with that found in other iron compounds. In $FeNbO_4$, the Fermi level, and hence the flat-band potential, is determined principally by the Fe^{3+}–Fe^{2+} hopping energies, whereas only the Nb^{5+}–Nb^{4+} states exist in the other two niobates.

The lowest, optical band gap at 2.08(2) eV can be attributed to the $[FeO_6]$ photoactive centers. However, three of the higher-energy band gaps agree closely with values obtained for the $[NbO_6]$ centers in $Ba_{0.5}Sr_{0.5}Nb_2O_6$. This result strongly implies the additive superposition of multiple photoactive centers, rather than the "averaging" process suggested by conventional band theory. In conjunction with the difference between these energy gaps and those observed for $[NbO_6]$ centers in $Sr_2Nb_2O_7$, where all the *A* sites are filled, this result also indicates that *A*-site occupancy may be a significant factor.

It is interesting to note that the very weak band "tail" of $Ba_{0.5}Sr_{0.5}Nb_2O_6$ at 2.6(1) eV appears significantly strengthened in $FeNbO_4$. There is evidently an enhancement of the quantum efficiency due to the presence of $[FeO_6]$ active centers while retaining the fundamental energy characteristics of the $[NbO_6]$ octahedra.

Acknowledgments

The Office of Naval Research, Arlington, Virginia, supported the work of John Koenitzer, Bijan Khazai, and Kirby Dwight. Acknowledgment is made to the Solar Energy Research Institute, Golden, Colorado, for the support of Jacob Hormadaly. In addition, the authors would like to acknowledge the support of the Materials Research Laboratory Program at Brown University. The authors also wish to express their thanks to Dr. Lothar Brixner of E. I. DuPont de Nemours & Company, Wilmington, Delaware, for several helpful discussions.

References

1. J. Hormadaly, S. N. Subbarao, R. Kershaw, K. Dwight, and A. Wold, *J. Solid State Chem.* **33**, 27 (1980).
2. A. F. Wells, "Structural Inorganic Chemistry," 4th ed., p. 48, Oxford Univ. Press (Clarendon), London, (1975).
3. A. C. Turnock, *J. Amer. Ceram. Soc.* **49**, 4, 177 (1966).
4. Van der Pauw, L. J., *Phillips Res. Rep.* **16**, 187 (1961).
5. C. A. Ackert and J. Volger, *Phys. Lett.* **8**, 244 (1964).
6. S. N. Subbarao, Y. H. Yun, R. Kershaw, K. Dwight, and A. Wold, *Inorg. Chem.* **18**, 488 (1979).
7. H. H. Kung, H. S. Jarrett, A. W. Sleight, and A. Ferretti, *J. Appl. Phys.* **48**, 2463 (1977).
8. A. Nozik, *Annu. Rev. Phys. Chem.* **29**, 189 (1978).
9. F. P. Koffyberg, K. Dwight, and A. Wold, *Solid State Commun.* **30**, 433 (1979).